THE JOURNAL OF PHYSICAL CHEMISTRY B

Article

pubs.acs.org/JPCB

Dissolution of Cellulose in Room Temperature Ionic Liquids: Anion Dependence

Rajdeep Singh Payal,[†,‡] Karteek K. Bejagam,[†,‡] Anirban Mondal,[†] and Sundaram Balasubramanian*[,†]

[†]Chemistry and Physics of Materials Unit, Jawaharlal Nehru Centre for Advanced Scientific Research, Bangalore 560 064, India

Supporting Information

ABSTRACT: The dissolution of cellulosic biomass in room temperature ionic liquids (RTILs) is studied through free energy calculations of its monomer, viz., cellobiose, within a molecular dynamics simulation approach. The solvation free energy (SFE) of cellobiose in ionic liquids containing any of seven different anions has been calculated. The ranking of these liquids based on SFE compares well with experimental data on the solubility of cellulose. The dissolution is shown to be enthalpically dominated, which is correlated with the strength of intermolecular hydrogen bonding between cellobiose and the anions of the IL. Large entropic changes upon solvation in $[CF_3SO_3]^-$ and $[OAc]^-$ based ionic liquids have been explained in terms of the solvent-aided conformational flexibility of cellobiose.

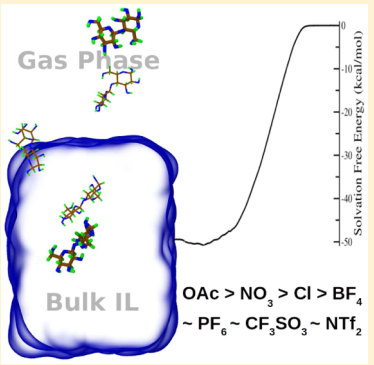

INTRODUCTION

Lignocellulosic biomass is a potential source of biofuel which can be converted into ethanol. However, one of the challenging task in this process is its dissolution. While cellulose is a crystalline polymer, other components of wood, i.e., hemicellulose and lignin, are amorphous.[1] The crystalline nature of the former arises from strong inter- and intramolecular hydrogen bonding between its monomers, i.e., cellobiose. These are covalently bonded to one another by $\beta(1-4)$ linkages to form long polymeric units. Conventional solvents such as water or benzene are unable to dissolve cellulose, and the process requires harsh conditions such as acid pretreatment and high temperature.[2]

This issue was addressed by Rogers et al. in 2002, who successfully dissolved cellulose in room temperature ionic liquids (RTIL) at relatively mild conditions.[3] They were also able to regenerate cellulose by addition of water or simple solvents. This discipline has seen a large amount of activity since then.[1,4−28]

NMR spectroscopy has been effectively employed to understand the dissolution mechanism of cellulose in ionic liquids.[29] The disruption of the inter- and intramolecular hydrogen bonding network of cellulose polymer in ILs was identified as key to its dissolution, and the anion was shown to be chiefly responsible. In most ILs, the cation is bulkier and acts only as a weak hydrogen bond (H-bond) donor and thus its role is not as significant as that of the anion. A recent NMR study by Zhang et al.[30] showed that cations too can form H-bonds with cellulose, albeit weaker ones.

Molecular modeling of room temperature ionic liquids has matured to a considerable extent.[31−35] There have been many attempts to understand the dissolution mechanism of lignocellulosic biomass in ionic liquids through theoretical methods.[36−38] Both empirical force field and ab initio based methods have been employed.[39−42] These studies also showed the weakening/disruption of the inter- and intramolecular hydrogen bond network in polymeric cellulose in various ILs. Examining the specific role of the ions, Zhao et al.[43,44] suggested the following attributes for better dissolution: (i) ions with less steric hindrance and (ii) anions with high electronegativity and without any electron withdrawing group. Our quantum cluster calculations[45] and density functional theory (DFT) based ab initio MD simulations[46] have investigated the disruption of intramolecular H-bonds and the dependence of the conformation of cellobiose on solvation.

Future development toward the choice of novel anions demands a comprehensive rationalization of experimental observations. In ILs, anions not only play a vital role in influencing the intermolecular structure[47] but also are important in determining solubilities of various solutes. Crucial solute−solvent interactions responsible for the dissolution of the polymer can be understood by carrying out studies on the solvation environment of the monomer. Thus, far, the free energy of solvation of model cellulose has not been examined in the literature. The current work is aimed at calculating the solvation free energy of a monomer of cellulose, i.e., cellobiose and its dependence on the anion of the ILs. It is also carried out to obtain a microscopic understanding of the experimental observation that the acetate anion is the most suited for this process. The calculations have been performed in the thermodynamically most stable conformational state of the cellobiose, anti-anti, an observation which too has been established here. Anticipating our results, we find the IL with

Received: December 9, 2014
Published: December 23, 2014

DOI: 10.1021/jp512240t
J. Phys. Chem. B 2015, 119, 1654−1659

the acetate anion to be the most suited for cellobiose solvation in terms of the magnitude of change in its free energy from gas phase, upon solvation. We suggest a choice of anions which could potentially enhance cellulose solubility.

COMPUTATIONAL DETAILS

Ionic liquids containing the [bmim] cation and any of the following anions were studied: $[OAc]^-$, $[NO_3]^-$, $[Cl]^-$, $[BF_4]^-$, $[PF_6]^-$, $[CF_3SO_3]^-$, and $[NTf_2]^-$. The conformational free energy profile of cellobiose in these ILs was studied in a system containing 100 ion pairs, while its solvation free energy was studied in systems containing 256 ion pairs. Cellobiose was modeled using the OPLS force field for carbohydrates[48] while ILs were modeled using the all-atom force field developed by Mondal and Balasubramanian.[49]

Three-dimensional periodic boundary conditions were employed. Tail corrections to energy and pressure were applied. Long range electrostatic interactions were evaluated using the particle−particle particle−mesh (PPPM) solver.[50] All the simulations were done at 353 K. The higher than ambient temperature was necessitated to include results from liquid [bmim][Cl] [m. pt. 343 K]. Furthermore, such temperatures are routinely employed in experiments (see Table 3 of ref 1) Temperature and pressure were maintained using a Nosé−Hoover thermostat and barostat, respectively.[51,52] Simulation trajectories were visualized and snapshots were rendered using VMD.[53]

The two stable conformers of cellobiose are anti-anti and anti-syn (Figure S1 of the Supporting Information), which can be distinguished by the torsional state of the two CH_2OH groups in the cellobiose.

Free energy calculations. All the FE simulations were carried out using the colvars module[54] embedded in LAMMPS.[55] The Adaptive Biasing Force (ABF)[56] method was used to determine the FE profiles.The span of the reaction coordinate (RC) was divided into bins in which accumulation of force takes place.

Conformational free energy. Cellobiose was solvated in a cubic box containing 100 ionic liquid molecules and equilibrated in the isothermal−isobaric (NPT) ensemble. The FE barrier across the C−C−C−O (see Figure 1) torsion was determined using the ABF method. RC was spanned from −180° to 180° with a bin width of 5°. FE calculations using the dihedral angle as the reaction coordinate were carried out for 100 ns in the NPT ensemble. ABF forces were applied every 500 steps.

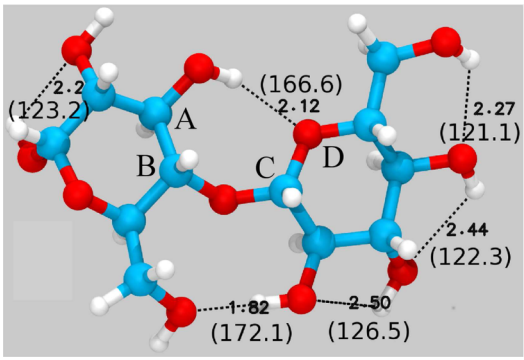

Figure 1. Atoms of cellobiose (labeled A, B, C, D) involved in the definition of the torsion angle, ϕ. Intramolecular H-bonds in the anti−anti conformer of cellobiose. Bond lengths and angles are in Å and deg, respectively. Color scheme: C, cyan; O, red; H, white.

Solvation free energy (SFE). SFE is the energy required to bring one cellobiose molecule from the gas phase into the bulk ionic liquid. 256 ion pairs were equilibrated in the NPT ensemble (P = 1 atm, T = 353 K). Later, simulations were carried out in the canonical ensemble (NVT), after increasing the box-length along the Z direction to a value of 150 Å, so as to create two liquid−vapor interfaces, which was followed by FE calculations in the NVT ensemble. Colvar style "distance Z" was used in determining the SFE profiles. RC was defined as the distance between the center of mass of ionic liquid molecules and the center of mass of cellobiose. It was divided into five nonoverlapping windows spanning from 7 to 50 Å along the Z direction such that cellobiose is completely immersed at 7 Å and completely in the gas-phase at 50 Å (see Figure S2 in the Supporting Information). Force samples were collected for 500 steps with bin width of 0.2 Å. Each window was run for at least 30 ns so as to achieve a sampling ratio between the highest and lowest points, of around 5.

SFE could have also been calculated using the Bennet acceptance ratio (BAR)[57] or expanded ensemble[58,59] methods. But, we adopted the equally facile ABF method here.

RESULTS AND DISCUSSION

Conformational free energy. Figure 1 displays the molecule in its anti-anti conformation and illustrates two categories of intramolecular H-bonds: (i) longer and bent and (ii) shorter and linear. The conformational free energy profile of cellobiose across ϕ in the gas phase is shown in Figure 2(a). A minimum in the free energy occurs at −25°, corresponding to its anti-anti state. This conformer is nearly planar and contains five intramolecular H-bonds, two of which are stronger than the other three. Two other minima are seen at 160° and −165°, which correspond to the anti-syn state of cellobiose. This conformer possesses four intramolecular H-bonds, of which two are stronger than the rest. The nonplanar conformer is thus less stable than the anti-anti one. The two maxima at 110° and −120° correspond to states where the hexose rings are nearly perpendicular to each other.

Figure 2(b) shows the conformational free energy (FE) profiles of cellobiose soaked in IL. The anti-anti configuration of cellobiose is more stable than the anti-syn one even when it is solvated in any IL. However, the torsional angle at which the free energy is a minimum shifts to a lower value (more negative) than what it was in the gas phase. In fact, the extent of shift in a specific ionic liquid is correlated with the potential energy change (ΔU) associated with solvation (see later). The shift is caused due to the breaking of intramolecular H-bonds of cellobiose and consequent formation of intermolecular H-bonds with solvent ions (see Table T1 in the Supporting Information). In fact, the anti-syn conformational state too gets shifted in solution. In most ILs, it is found at 140° and −160°. Two maxima are seen in the conformational FE profiles of solvated cellobiose. One of them is around 100° (shorter) and another is around −150° (taller). As compared to gas phase data (Figure 2(a)), the relative intensities of these maxima are observed to be swapped in the presence of IL. The change can be explained thus: the FE maximum at 100° occurs when the two hexose rings are almost perpendicular to each other. In this situation, most of the hydroxyl hydrogen atoms are exposed to the solvent and can form H-bonds with solvent ions, which decreases the free energy of this state relative to its value in the

DOI: 10.1021/jp512240t
J. Phys. Chem. B 2015, 119, 1654−1659

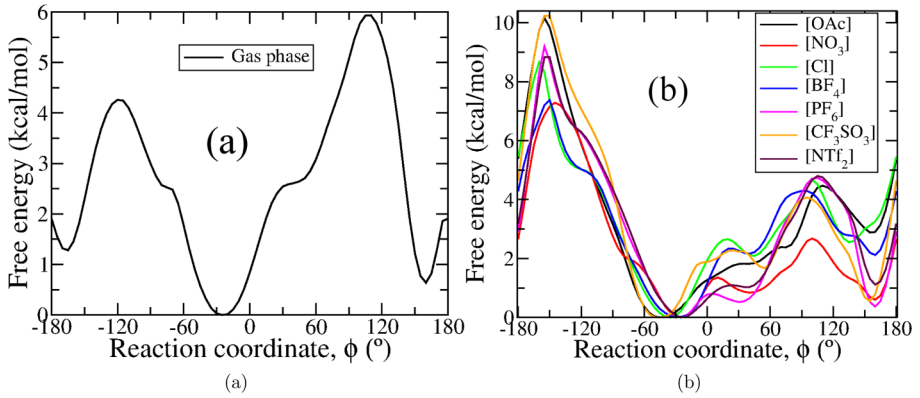

Figure 2. Conformational free energy of cellobiose (a) in the gas phase and (b) solvated in ionic liquids. Anions are shown in the legend, while the cation is [bmim]. T = 353 K.

gas phase. When $\phi = -145°$, none of the hydroxyl hydrogens are able to form either intra- or intermolecular H-bonds, leading to a high FE barrier.

Again, two kinds of H-bonds can be formed between cellobiose and IL: viz. one between the anion of IL and the hydroxyl hydrogen of cellobiose (stronger) and a second between the cation of IL and the oxygen of cellobiose (relatively weaker). In general, the former are more in number than the latter. These results are in good agreement with our previous works.[45,46] In [emim][OAc], all intramolecular H-bonds of cellobiose in its anti-syn state were found to be broken, while the anti-anti state retains one or two such H-bonds.[46] Figure S3 and S4 (Supporting Information) display snapshots of H-bonds formed between cellobiose and the ions in [bmim][OAc] and [bmim][NTf_2].

Solvation free energy. Conformational free energy profiles of cellobiose solvated in various ionic liquids have unambiguously shown the greater stability of the anti-anti conformer over the anti-syn one. Thus, the question of relative stability and consequently the solubility of cellobiose in different ionic liquids can be addressed now. The free energy profiles for bringing the solute, cellobiose, from its vapor phase into the IL have thus been calculated using its anti-anti conformer. Needless to state, cellobiose was not constrained to be present in this conformation during the free energy simulations. However, once initiated from this torsional state, the same remained invariant (within fluctuations) during the simulations (Figure S5 of Supporting Information). Figure 3 displays solvation free energy profiles in various ILs containing

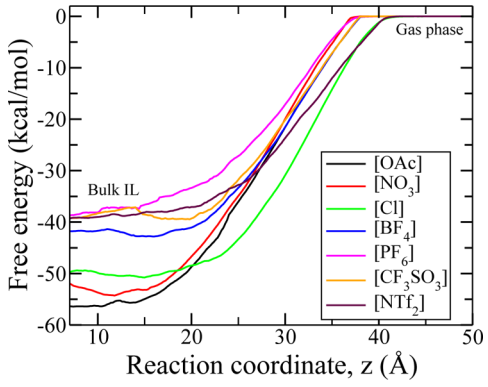

Figure 3. Solvation free energy of cellobiose in various ionic liquids, at 353 K. The cation is [bmim].

the same cation but different anions. The difference in the free energies between the vapor (gas phase) and the solvated state is the solvation free energy (SFE) of cellobiose in that particular IL. SFE is highest for [bmim][OAc] and lowest for [bmim][PF_6]. Moving in from the gas phase, the SFE profiles in most ILs become nonzero at around 38 Å. However, in the cases of [bmim][Cl] and [bmim][NTf_2], such changes appear at 41 Å itself. In [bmim][NTf_2], this is due the larger width of the density profile (see Figure S6 of the Supporting Information), while in [bmim][Cl], this is due to the movement of a few chloride ions from the liquid phase toward cellobiose (see Figure S7 of the Supporting Information).

Given that the liquid slab is in equilibrium with its vapor phase, one can assume the system to be at zero pressure, and thus changes in potential energy can be assumed to be identical to that in enthalpy. Enthalpic contributions to the relative stability of cellobiose in different ILs can be interpreted in terms of the strength of the intermolecular H-bonds. $[OAc]^-$, $[NO_3]^-$, and $[Cl]^-$ anions form strong H-bonds with cellobiose. Solvation free energies in [bmim][NTf_2], [bmim]-[CF_3SO_3], and [bmim][PF_6] are comparable, as the H-bonding strengths of their anions are nearly the same. [bmim][BF_4] exhibits an intermediate behavior. This behavior is also observed in the radial distribution function between the hydroxyl hydrogen of cellobiose and the H-bonding site of the anion (Figure 4). The first peak for $[OAc]^-$, $[NO_3]^-$, and $[Cl]^-$ is present at 1.8 Å, whereas for $[NTf_2]^-$, $[CF_3SO_3]^-$, and $[PF_6]^-$, it is at 2.10 Å. In the case of $[BF_4]^-$, the peak position is at 2.0 Å. The trend in the SFE is similar to that exhibited by the binding energy of one ion pair of any IL with cellobiose (Figure S8 of the Supporting Information shows the optimized configuration of cellobiose with an IL ion pair). Table T2 (Supporting Information) provides BE of cellobiose with ion pairs in the gas phase. A correlation between the BE in the gas phase and SFE can be established, which is displayed in Figure 5, which suggests an enthalpic basis for cellulose dissolution.

A breakup of the solvation free energy into its energetic and entropic contributions is vital to understand its anion dependence. Figure 6 provides the free energy and potential energy profiles for the system of cellobiose and [bmim][Cl]. The latter includes both cellobiose−IL and IL−IL interactions. Such a dissection of contributions to the free energy profile across a liquid−vapor interface has earlier been presented in ref 60. Similar profiles were calculated for all the liquids. Interestingly, the potential energy profile shows a small barrier at the liquid−vapor interface, which likely arises from the

DOI: 10.1021/jp512240t
J. Phys. Chem. B 2015, 119, 1654−1659

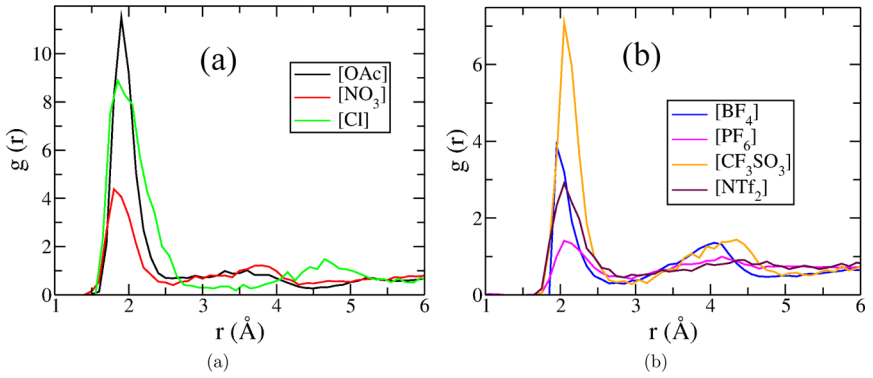

Figure 4. Radial distribution function between the hydroxyl hydrogen of cellobiose and the hydrogen bonding sites of anions.

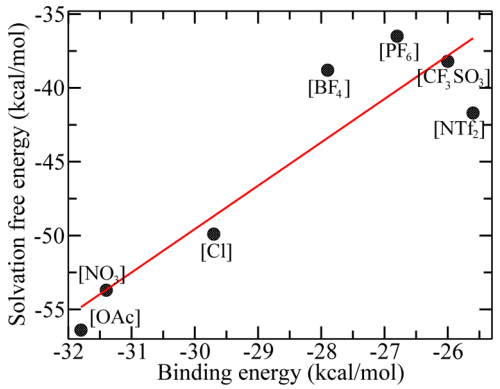

Figure 5. Binding energy of cellobiose with the ion pair where [bmim] is the cation versus the solvation free energy of cellobiose in bulk ionic liquid. The line is the best fit for the data, and positive slope indicates that the dissolution is determined by the enthalpic contribution.

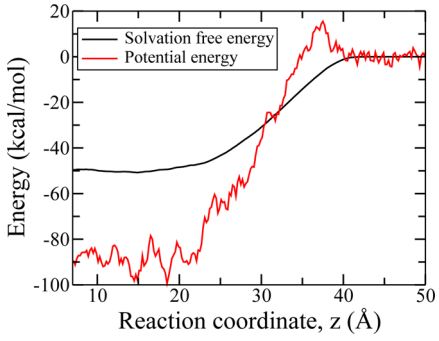

Figure 6. Solvation free energy and potential energy profiles of cellobiose in [bmim][Cl]. The two curves have been plotted by considering the respective gas phase values as reference. The difference between the two curves is the entropic contribution.

repulsive interaction between cellobiose and the butyl tails of the cation preferentially oriented normal to the interface. A similar barrier was present in the potential energy vs RC profiles in all ILs. In bulk IL, the cellobiose is well solvated by the ions, which leads to a large, negative potential energy. The difference between the solvation free energy and the potential energy equals the entropy change (times the temperature) upon solvation. The same has been calculated for cellobiose dissolution in different ILs and is presented in Table 1.

In the case of [bmim][OAc], [bmim][NO_3], and [bmim]-[Cl], the energy differences are relatively high whereas the entropic contribution is moderate. Hence, the solvation free energy of cellobiose is higher in these liquids than in others. In [bmim][CF_3SO_3], both energy and entropy differences are high, and as a result, the net solvation free energy is low. In other ILs, both energy and entropy contributions are moderate, causing the poor solubility of cellobiose in these ILs. Among the ILs studied here, the dissolution of cellulose is most facile in [bmim][OAc], as determined experimentally. The calculated SFE for cellobiose in [bmim][OAc] being the most negative (among ILs studied here) is consistent with the experimental observation and offers a microscopic understanding of its dissolution.

Table 1. Change in the Free Energy ($\Delta A = A_{liq} - A_{gas}$), Potential Energy ($\Delta U = U_{liq} - U_{gas}$), and Entropy Contribution ($T\Delta S = S_{liq} - S_{gas}$) for the Dissolution of Cellobiose in Various ILs Relative to Its Gas Phase[a]

IL	ΔA (kcal/mol)	ΔU (kcal/mol)	$T\Delta S$ (kcal/mol)	$T\Delta S/\Delta U$
[OAc]	−56.4	−113.8	−57.4	0.5
[NO_3]	−53.7	−84.1	−30.3	0.3
[Cl]	−49.9	−87.4	−37.4	0.4
[BF_4]	−41.7	−78.5	−36.7	0.4
[PF_6]	−36.5	−64.7	−28.1	0.4
[CF_3SO_3]	−38.2	−127.0	−88.7	0.7
[NTf_2]	−38.8	−71.1	−32.3	0.4

[a][bmim]$^+$ is the cation.

Figure 7 shows the distribution of the angle between the normal vectors of the hexose rings of cellobiose. The distributions in [bmim][OAc] and [bmim][CF_3SO_3] are much broader than those in other ILs. They are also compared

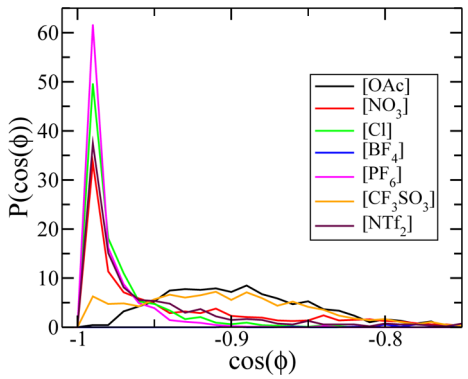

Figure 7. Distribution of the angle between the the two hexose ring planes of cellobiose in various ILs.

DOI: 10.1021/jp512240t
J. Phys. Chem. B 2015, 119, 1654−1659

against the distributions in gas phase cellobiose in Figure S9 (Supporting Information). The larger width in these two ILs indicates the facile deviation from the planar geometry of cellobiose; it is also consistent with the high entropy difference ($T\Delta S$) in these two ionic liquids. The nonplanar geometry is also responsible for the high enthalpy values, as it allows for the formation of intermolecular hydrogen bonds at the expense of intramolecular ones. The larger width in the case of the above-mentioned two ILs can also be associated with the size and symmetry of the anion. $[OAc]^-$ and $[CF_3SO_3]^-$ are less symmetric and bulkier as compared to other anions. Thus, the hexose rings of cellobiose will be farther apart in order for its hydroxyl hydrogens to form H-bonds with such anions, resulting in a broader distribution of the interhexose angle in such ILs.

CONCLUSIONS

In summary, our simulations show that a high enthalpy difference with a moderate entropic contribution appears to be vital in determining the solubility of cellulosic biomass in room temperature ionic liquids. A good solvent is one which contains a strong H-bond acceptor and a moderate H-bond donor. Anions have earlier been implicated to play an crucial role in cellulose dissolution, and the same has been examined here. Experimentally determined solubility of cellulose in ILs varies as $[OAc]^- > [Cl]^- > [BF_4]^- \sim [PF_6]^-$.[1,3] SFE values calculated here are consistent with the experimental observations. In particular, the large entropic contribution to free energy in $[OAc]^-$ and $[CF_3SO_3]^-$ based ionic liquids has been demonstrated to originate from the conformational flexibility of cellobiose in these systems.

The disruption of the inter- and intramolecular hydrogen bonding network of cellulose is the key to its dissolution mechanism. Fluorine in $[CF_3SO_3]$ makes it less basic due to its electron withdrawing nature. Replacing fluorine atoms with hydrogen can make it a better hydrogen bond acceptor. Methylsulfonate anion could also be explored as anion. Also, the reduction in the size of the anion will result in less steric hindrance and can also improve the solubility of cellulose in ionic liquids.

ASSOCIATED CONTENT

Supporting Information

Table and figures of the hydrogen bonding environment of cellobiose in ionic liquids, the two most stable conformers of cellobiose in the gas phase, schematic of reaction coordinate for determining solvation free energy, conformational states of cellobiose in gas phase and in bulk IL, mass and number density profiles of ionic liquids, values of binding energies of ion pair with cellobiose, distribution of angle between ring normals of cellobiose in gas phase and bulk IL (OAc and CF_3SO_3). This material is available free of charge via the Internet at http://pubs.acs.org.

AUTHOR INFORMATION

Corresponding Author

*E-mail: bala@jncasr.ac.in.

Author Contributions

‡R.S.P. and K.K.B. contributed equally.

Notes

The authors declare no competing financial interest.

ACKNOWLEDGMENTS

R.S.P. and K.K.B. thank CSIR for a Senior Research Fellowship. We thank DST for support. S.B. thanks the Sheikh Saqr Laboratory for a senior fellowship.

REFERENCES

(1) Sun, N.; Rodríguez, H.; Rahman, M.; Rogers, R. D. Where are Ionic Liquid Strategies Most Suited in the Pursuit of Chemicals and Energy from Lignocellulosic Biomass? *Chem. Commun.* **2011**, *47*, 1405−1421.

(2) Nishino, T.; Matsuda, I.; Hirao, K. All-Cellulose Composite. *Macromolecules* **2004**, *37*, 7683−7687.

(3) Swatloski, R. P.; Spear, S. K.; Holbrey, J. D.; Rogers, R. D. Dissolution of Cellose with Ionic Liquids. *J. Am. Chem. Soc.* **2002**, *124*, 4974−4975.

(4) Zhu, S.; Wu, Y.; Chen, Q.; Yu, Z.; Wang, C.; Jin, S.; Ding, Y.; Wu, G. Dissolution of Cellulose with Ionic Liquids and its Application: A Mini-review. *Green Chem.* **2006**, *8*, 325−327.

(5) Pinkert, A.; Marsh, K. N.; Pang, S.; Staiger, M. P. Ionic Liquids and Their Interaction with Cellulose. *Chem. Rev.* **2009**, *109*, 6712−6728.

(6) Wang, H.; Gurau, G.; Rogers, R. D. Ionic Liquid Processing of Cellulose. *Chem. Soc. Rev.* **2012**, *41*, 1519−1537.

(7) Sun, N.; Rahman, M.; Qin, Y.; Maxim, M. L.; Rodriguez, H.; Rogers, R. D. Complete Dissolution and Partial Delignification of Wood in the Ionic Liquid 1-ethyl-3-methylimidazolium Acetate. *Green Chem.* **2009**, *11*, 646−655.

(8) Brandt, A.; Hallett, J. P.; Leak, D. J.; Murphy, R. J.; Welton, T. The Effect of the Ionic Liquid Anion in the Pretreatment of Pine Wood Chips. *Green Chem.* **2010**, *12*, 672−679.

(9) Fort, D. A.; Remsing, R. C.; Swatloski, R. P.; Moyna, P.; Moyna, G.; Rogers, R. D. Can Ionic Liquids Dissolve Wood? Processing and Analysis of Lignocellulosic Materials with 1- *n*-butyl-3-methylimidazolium Chloride. *Green Chem.* **2007**, *9*, 63−69.

(10) Zhao, B.; Greiner, L.; Leitner, W. Cellulose Solubilities in Carboxylate-based Ionic Liquids. *RSC Adv.* **2012**, *2*, 2476−2479.

(11) Ohno, H.; Fukaya, Y. Task Specific Ionic Liquids for Cellulose Technology. *Chem. Lett.* **2009**, *38*, 2−7.

(12) Hummel, M.; Froschauer, C.; Laus, G.; Röder, T.; Kopacka, H.; Hauru, L. K.; Weber, H. K.; Sixta, H.; Schottenberger, H. Dimethyl Phosphorothioate and Phosphoroselenoate Ionic Liquids as Solvent Media for Cellulosic Materials. *Green Chem.* **2011**, *13*, 2507−2517.

(13) Zhao, H.; Jones, C. L.; Baker, G. A.; Xia, S.; Olubajo, O.; Person, V. N. Regenerating Cellulose from Ionic Liquids for an Accelerated Enzymatic Hydrolysis. *J. Biotechnol.* **2009**, *139*, 47−54.

(14) Moulthrop, J. S.; Swatloski, R. P.; Moyna, G.; Rogers, R. D. High-resolution ^{13}C NMR Studies of Cellulose and Cellulose Oligomers in Ionic Liquid Solutions. *Chem. Commun.* **2005**, 1557−1559.

(15) Li, W.; Sun, N.; Stoner, B.; Jiang, X.; Lu, X.; Rogers, R. D. Rapid Dissolution of Lignocellulosic Biomass in Ionic Liquids Using Temperatures Above the Glass Transition of Lignin. *Green Chem.* **2011**, *13*, 2038−2047.

(16) Freire, M. G.; Teles, A. R. R.; Rocha, M. A.; Schroder, B.; Neves, C. M.; Carvalho, P. J.; Evtuguin, D. V.; Santos, L. M.; Coutinho, J. A. Thermophysical Characterization of Ionic Liquids Able to Dissolve Biomass. *J. Chem. Eng. Data* **2011**, *56*, 4813−4822.

(17) Vancov, T.; Alston, A.-S.; Brown, T.; McIntosh, S. Use of Ionic Liquids in Converting Lignocellulosic Material to Biofuels. *Renewable Energy* **2012**, *45*, 1−6.

(18) Binder, J. B.; Raines, R. T. Fermentable Sugars by Chemical Hydrolysis of Biomass. *Proc. Natl. Acad. Sci.* **2010**, *107*, 4516−4521.

(19) Brandt, A.; Hallett, J. P.; Leak, D. J.; Murphy, R. J.; Welton, T. The Effect of the Ionic Liquid Anion in the Pretreatment of Pine Wood Chips. *Green Chem.* **2010**, *12*, 672−679.

(20) Zhang, H.; Wu, J.; Zhang, J.; He, J. 1-Allyl-3-methylimidazolium Chloride Room Temperature Ionic Liquid: A New and Powerful

DOI: 10.1021/jp512240t
J. Phys. Chem. B 2015, 119, 1654−1659

Nonderivatizing Solvent for Cellulose. *Macromolecules* **2005**, *38*, 8272−8277.
(21) Kosan, B.; Michels, C.; Meister, F. Dissolution and Forming of Cellulose with Ionic Liquids. *Cellulose* **2008**, *15*, 59−66.
(22) Zakrzewska, M. E.; Bogel-Łukasik, E.; Bogel-Łukasik, R. Solubility of Carbohydrates in Ionic Liquids. *Energy Fuels* **2010**, *24*, 737−745.
(23) Wishart, J. F. Energy Applications of Ionic Liquids. *Energy Environ. Sci.* **2009**, *2*, 956−961.
(24) Xie, H.; King, A.; Kilpelainen, I.; Granstrom, M.; Argyropoulos, D. S. Thorough Chemical Modification of Wood-based Lignocellulosic Materials in Ionic Liquids. *Biomacromolecules* **2007**, *8*, 3740−3748.
(25) Samayam, I. P.; Hanson, B. L.; Langan, P.; Schall, C. A. Ionic-liquid Induced Changes in Cellulose Structure Associated with Enhanced Biomass Hydrolysis. *Biomacromolecules* **2011**, *12*, 3091−3098.
(26) Li, B.; Asikkala, J.; Filpponen, I.; Argyropoulos, D. S. Factors Affecting Wood Dissolution and Regeneration of Ionic Liquids. *Ind. Eng. Chem. Res.* **2010**, *49*, 2477−2484.
(27) Shen, T.; Langan, P.; French, A. D.; Johnson, G. P.; Gnanakaran, S. Conformational Flexibility of Soluble Cellulose Oligomers: Chain Length and Temperature Dependence. *J. Am. Chem. Soc.* **2009**, *131*, 14786−14794.
(28) Gao, D.; Chundawat, S. P.; Sethi, A.; Balan, V.; Gnanakaran, S.; Dale, B. E. Increased Enzyme Binding to Substrate is Not Necessary for More Efficient Cellulose Hydrolysis. *Proc. Natl. Acad. Sci.* **2013**, *110*, 10922−10927.
(29) Remsing, R. C.; Swatloski, R. P.; Rogers, R. D.; Moyna, G. Mechanism of Cellulose Dissolution in the Ionic Liquid 1- *n*-butyl-3-methylimidazolium Chloride: a ^{13}C and $^{35/37}Cl$ NMR relaxation study on model systems. *Chem. Commun.* **2006**, 1271−1273.
(30) Zhang, J.; Zhang, H.; Wu, J.; Zhang, J.; He, J.; Xiang, J. NMR Spectroscopic Studies of Cellobiose Solvation in EmimAc Aimed to Understand the Dissolution Mechanism of Cellulose in Ionic Liquids. *Phys. Chem. Chem. Phys.* **2010**, *12*, 1941−1947.
(31) Shah, J. K.; Maginn, E. J. *Molecular Simulation of Ionic Liquids: Where We are and the Path Forward*; John Wiley & Sons, Inc.: 2014; pp 149−192.
(32) Choi, E.; McDaniel, J. G.; Schmidt, J. R.; Yethiraj, A. First-Principles, Physically Motivated Force Field for the Ionic Liquid [BMIM][BF_4]. *J. Phys. Chem. Lett.* **2014**, *5*, 2670−2674.
(33) Chaban, V. V.; Prezhdo, O. V. Ionic and Molecular Liquids: Working Together for Robust Engineering. *J. Phys. Chem. Lett.* **2013**, *4*, 1423−1431.
(34) Chaban, V. V.; Prezhdo, O. V. Computationally Efficient Prediction of Ionic Liquid Properties. *J. Phys. Chem. Lett.* **2014**, *5*, 1973−1977.
(35) Liu, Z.; Chen, T.; Bell, A.; Smit, B. Improved United-Atom Force Field for 1-alkyl-3-methylimidazolium Chloride. *J. Phys. Chem. B* **2010**, *114*, 4572−4582.
(36) Youngs, T. G. A.; Hardacre, C.; Holbrey, J. D. Glucose Solvation by the Ionic Liquid 1,3-dimethylimidazolium Chloride: A Simulation Study. *J. Phys. Chem. B* **2007**, *111*, 13765−13774.
(37) Youngs, T. G.; Holbrey, J. D.; Deetlefs, M.; Nieuwenhuyzen, M.; Costa Gomes, M. F.; Hardacre, C. A Molecular Dynamics Study of Glucose Solvation in the Ionic Liquid 1, 3-dimethylimidazolium Chloride. *ChemPhysChem* **2006**, *7*, 2279−2281.
(38) Liu, H.; Sale, K. L.; Holmes, B. M.; Simmons, B. A.; Singh, S. Understanding the Interactions of Cellulose with Ionic Liquids: A Molecular Dynamics Study. *J. Phys. Chem. B* **2010**, *114*, 4293−4301.
(39) Rabideau, B. D.; Agarwal, A.; Ismail, A. E. Observed Mechanism for the Breakup of Small Bundles of Cellulose Iα and Iβ in Ionic Liquids from Molecular Dynamics Simulations. *J. Phys. Chem. B* **2013**, *117*, 3469−3479.
(40) Janesko, B. G. Modeling Interactions Between Lignocellulose and Ionic Liquids Using DFT-D. *Phys. Chem. Chem. Phys.* **2011**, *13*, 11393−11401.
(41) Guo, J.; Zhang, D.; Duan, C.; Liu, C. Probing Anion Cellulose Interactions in Imidazolium-based Room Temperature Ionic Liquids: A Density Functional Study. *Carbohydr. Res.* **2010**, *345*, 2201−2205.
(42) Liu, C.; Guo, J.; Zhang, D. A Ttheoretical Investigation of the Interactions Between Cellulose and 1-butyl-3-methylimidazolium Chloride. *J. Theor. Comput. Chem.* **2010**, *09*, 611−624.
(43) Zhao, Y.; Liu, X.; Wang, J.; Zhang, S. Effects of Cationic Structure on Cellulose Dissolution in Ionic Liquids: A Molecular Dynamics Study. *ChemPhysChem* **2012**, *13*, 3126−3133.
(44) Zhao, Y.; Liu, X.; Wang, J.; Zhang, S. Effects of Anionic Structure on the Dissolution of Cellulose in Ionic Liquids Revealed by Molecular Simulation. *Carbohydr. Polym.* **2013**, *94*, 723−730.
(45) Payal, R. S.; Bharath, R.; Periyasamy, G.; Balasubramanian, S. Density Functional Theory Investigations on the Structure and Dissolution Mechanisms for Cellobiose and Xylan in an Ionic Liquid: Gas Phase and Cluster Calculations. *J. Phys. Chem. B* **2012**, *116*, 833−840.
(46) Payal, R. S.; Balasubramanian, S. Dissolution of Cellulose in Ionic Liquids: An Ab Initio Molecular Dynamics Simulation Study. *Phys. Chem. Chem. Phys.* **2014**, *16*, 17458−17465.
(47) Hettige, J. J.; Kashyap, H. K.; Annapureddy, H. V.; Margulis, C. J. Anions, the Reporters of Structure in Ionic Liquids. *J. Phys. Chem. Lett.* **2012**, *4*, 105−110.
(48) Damm, W.; Frontera, A.; Tirado-Rives, J.; Jorgensen, W. L. OPLS All-Atom Force Field for Carbohydrates. *J. Comput. Chem.* **1997**, *18*, 1955−1970.
(49) Mondal, A.; Balasubramanian, S. Quantitative Prediction of Physical Properties of Imidazolium Based Room Temperature Ionic Liquids through Determination of Condensed Phase Site Charges: A Refined Force Field. *J. Phys. Chem. B* **2014**, *118*, 3409−3422.
(50) Hockney, R. W.; Eastwood, J. W. *Computer Simulation Using Particles*; Adam Hilger: 1988.
(51) Nosé, S. A Unified Formulation of the Constant Temperature Molecular Dynamics Methods. *J. Chem. Phys.* **1984**, *81*, 511−519.
(52) Hoover, W. G. Canonical Dynamics: Equilibrium Phase-Space Distributions. *Phys. Rev. A* **1985**, *31*, 1695−1697.
(53) Humphrey, W.; Dalke, A.; Schulten, K. VMD—Visual Molecular Dynamics. *J. Mol. Graph.* **1996**, *14*, 33−38.
(54) Fiorin, G.; Klein, M. L.; Hénin, J. Using Collective Variables to Drive Molecular Dynamics Simulations. *Mol. Phys.* **2013**, *111*, 3345−3362.
(55) Plimpton, S. Fast Parallel Algorithms for Short-Range Molecular Dynamics. *J. Comput. Phys.* **1995**, *117*, 1−19.
(56) Darve, E.; Rodríguez-Gómez, D.; Pohorille, A. Adaptive Biasing Force Method for Scalar and Vector Free Energy Calculations. *J. Chem. Phys.* **2008**, *128*, 144120.
(57) Bennett, C. H. Efficient Estimation of Free Energy Differences from Monte Carlo Data. *J. Comput. Phys.* **1976**, *22*, 245−268.
(58) Paluch, A. S.; Shah, J. K.; Maginn, E. J. Efficient Solvation Free Energy Calculations of Amino Acid Analogs by Expanded Ensemble Molecular Simulation. *J. Chem. Theory Comput.* **2011**, *7*, 1394−1403.
(59) Paluch, A. S.; Mobley, D. L.; Maginn, E. J. Small Molecule Solvation Free Energy: Enhanced Conformational Sampling Using Expanded Ensemble Molecular Dynamics Simulation. *J. Chem. Theory Comput.* **2011**, *7*, 2910−2918.
(60) Otten, D. E.; Shaffer, P. R.; Geissler, P. L.; Saykally, R. J. Elucidating the Mechanism of Selective Ion Adsorption to the Liquid Water Surface. *Proc. Natl. Acad. Sci.* **2012**, *109*, 701−705.

DOI: 10.1021/jp512240t
J. Phys. Chem. B 2015, 119, 1654−1659